J Mater Sci (2008) 43:2778–2784
DOI 10.1007/s10853-008-2510-8

SnO_2@C core-shell spheres: synthesis, characterization, and performance in reversible Li-ion storage

Hui Qiao · Zhi Zheng · Lizhi Zhang · Lifen Xiao

Received: 30 October 2007 / Accepted: 29 January 2008 / Published online: 28 February 2008

Abstract The nanostructured SnO_2@C spheres with tin oxide cores and carbon shells were prepared by a facile one-pot solvothermal method followed by a subsequent calcination at 600 °C in a high-purity nitrogen atmosphere. The resulting samples were characterized with thermogravimetric analysis (TGA), X-ray diffraction (XRD), energy-dispersive spectroscopy (EDS), infrared spectroscopy (IR), X-ray photoelectron spectroscopy (XPS), field-emission scanning electron microscopy (FE-SEM), transmission electron microscopy (TEM), and charge-discharge test. Electrochemical performance test showed that these SnO_2@C core-shell spheres exhibited an initial discharge specific capacity of 667.4 mAh/g in the potential range of 1.2–0.01 V. After 18 cycles, the capacity of the SnO_2@C core-shell spheres anode stabilized reversibly at about 370 mAh/g. This improved cycling performance could be attributed to the carbon shells, which can enhance the conductivity of SnO_2 and suppress the aggregation of active particles to increase their structure stability during cycling. These SnO_2@C core-shell spheres are promising anodes for lithium ion batteries. This study provides a facile way to improve the cycle ability of transition oxides for reversible lithium-ion storage.

H. Qiao · L. Zhang · L. Xiao (✉)
Key Laboratory of Pesticide & Chemical Biology of Ministry of Education, College of Chemistry, Central China Normal University, Wuhan 430079, China
e-mail: lfxiao@mail.ccnu.edu.cn

Z. Zheng
Institute of Surface Micro and Nano Materials, Xuchang University, Xuchang 461000, China

Introduction

Since the introduction of commercial lithium-ion batteries for potable devices in the 1990s, the search for new anode materials to improve energy density has been ongoing. Graphite, with a theoretical capacity of 372 mAh/g [1, 2], is the standard anode material used in commercial lithium-ion batteries. SnO_2 has been considered as a potential graphite substitute primarily on the basis of its higher theoretical capacity (about 790 mAh/g). However, the practical application of SnO_2 is hampered by its poor cyclability arising from the large specific volume change (about 358%) in repetitive charging and discharging of the battery, which causes mechanical failure and loss of electrical contact at the anode [3–14]. Many efforts have been devoted to avoid the capacity fading. These efforts mainly include the synthesis of nanostructured SnO_2 materials and the utilization of matrixes. The nanostructure ensures that the SnO_2 region is small enough initially for a fast diffusion of lithium ions into the electrode, and prevents the SnO_2 particles to aggregate into larger and inactive SnO_2 clusters during cycling [15, 16]. While different matrixes with electronic and ionic conductivity can accommodate the large volume changes. Recently, it is found that matrix composed of carbonaceous materials can reduce the capacity fading to some extent [8, 17–21]. For example, the cycling performance of Sn [11, 20], SnO_2 [8, 13], Si [22, 23], TiO_2 [24], and NiO [25, 26] had been significantly enhanced by forming composite with carbon. This is because carbon can act as a barrier to suppress the aggregation of active particles and thus increase their structure stability during cycling [8, 20, 24–26], and also act as a buffering matrix to relax the expansion that occurred within the electrode upon lithiation/delithiation process [22, 23]. Furthermore, carbon has a high electronic conductivity and

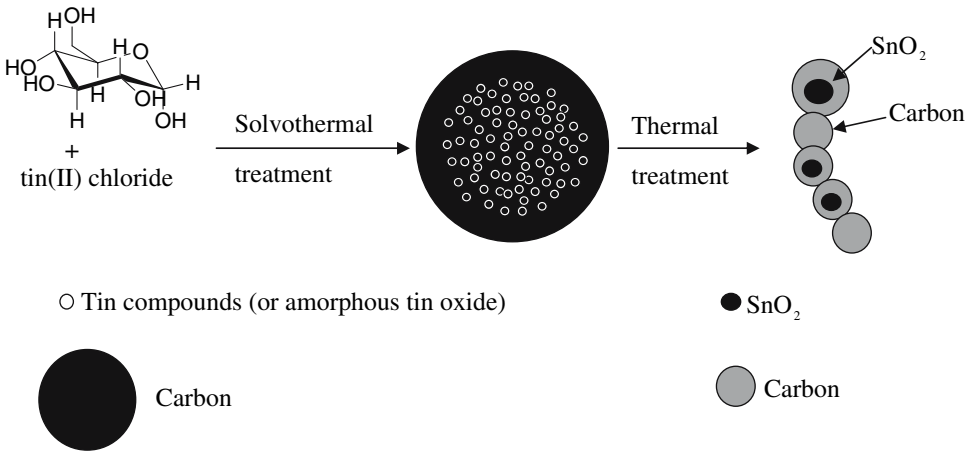

Scheme 1 Schematic illustration of the formation of SnO_2@C core-shell spheres

can improve the conductance of the active materials [13, 25, 26]. Therefore, the synthesis of composite electrodes with carbon is an effective way to improve the electrochemical performance of electrodes.

In this present work, we improved the cycling performance of SnO_2 by synthesizing SnO_2@C core-shell spheres via a facile solvothermal method followed by a subsequent calcination at 600 °C in a high-purity nitrogen atmosphere. Electrochemical characterization on SnO_2@C core-shell spheres exhibited an initial discharge capacity of 667.4 mAh/g and much better cyclability than that in the previous report [21] (Scheme 1).

Experimental

All chemical reagents used in this work were of analytical grade. In a typical experiment, 0.226 g of $SnCl_2{\cdot}2H_2O$ and 0.198 g of glucose hydrate were dissolved in 18 mL of anhydrous ethanol. The resulting solution was transferred into a 22-mL Teflon-sealed autoclave and then stored at 180 °C for 24 h, finally air-cooled to room temperature. The resulting product was washed with anhydrous ethanol thoroughly, and then dried at 60 °C in a vacuum-oven to obtain a dry powder. We denoted the dry powder as the as-prepared SC; subsequently, the as-prepared SC was calcined at 600 °C for 3 h in nitrogen atmosphere to obtain the final product, which was denoted as the annealed SC.

The crystalline structures and morphology of the products were recorded on an X-ray diffractometer with Cu-Kα radiation (MAC Science Co. Ltd. MXP 18 AHF), a Field-emission scanning electron microscope (JSM-5600), and a transmission electron microscopy (Philip CM 120), respectively. Thermogravimetric measurement was conducted on a TGA 2050 analyzer under an airflow of 100 mL/min with a heating rate of 10 °C/min from room temperature to 800 °C. Infrared spectra were measured on the Fourier infrared spectrum instrument (Nicolet Magna-IR 750). XPS measurements were performed in a VG Scientific ESCALAB Mark II spectrometer equipped with two ultra-highvacuum (UHV) chambers. All the binding energies were calibrated to the C1s peak at 284.8 eV of the surface adventitious carbon.

The testing cells had a typical two-electrode construction. The working electrodes were prepared by coating a copper foil substrate with the slurry of the active materials (80 wt.%), carbon black (10 wt.%), and poly(vinylidene fluoride) (10 wt.%) dissolved in cyclopentanone. After coating, the slurry was dried at 100 °C for 12 h and then pressed between two stainless steel plates at 1 MPa. The counter electrodes were lithium sheets. The separator was Celgard microporous membrane. The electrolyte was 1 M $LiPF_6$ dissolved in a 1:1 mixture (by weight) of ethylene carbonate (EC) and diethyl carbonate (DEC). The cells were assembled in an argon-filled glovebox. Charge-discharge tests were carried out at 30 mA/g using a battery charger between 1.2 and 0.01 V vs. Li/Li^+.

Results and discussion

XRD patterns and EDS spectrum

The X-ray diffraction pattern was used to characterize the atomic structure of the products. Figure 1 shows the typical XRD patterns of as-prepared and annealed SC samples. From Fig. 1a, we can see that the as-prepared sample has poor crystallinity. After annealed at 600 °C in N_2 atmosphere, the resulting sample possesses very good crystallinity (Fig. 1b). All the diffraction peaks of the annealed SC can be well indexed to tetragonal SnO_2 (JCPDS, No. 41-1445). No XRD peak from carbon suggested the amorphous structure of carbon. EDS analysis of the as-prepared SC sample confirmed the coexistence of carbon, oxygen, and

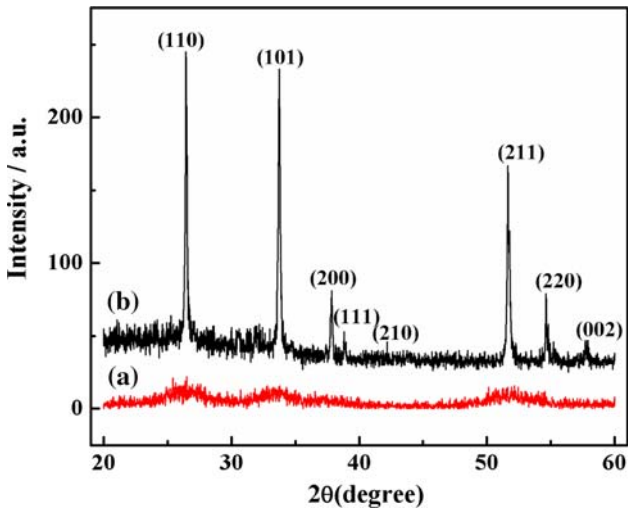

Fig. 1 XRD patterns of (**a**) as-prepared SC sample and (**b**) the SC sample after calcined at 600 °C for 3 h in nitrogen atmosphere

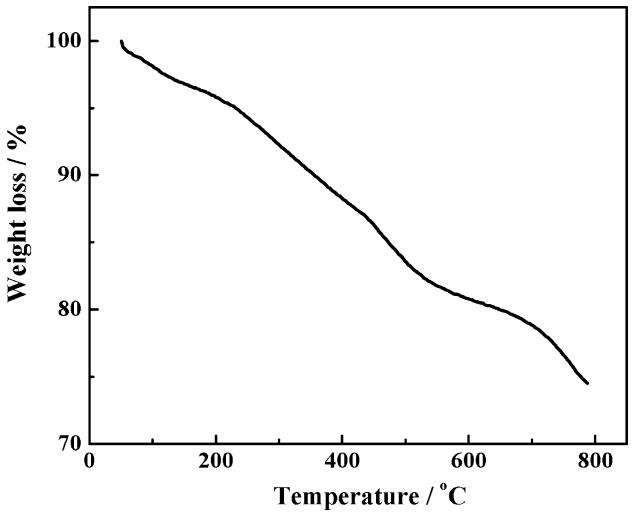

Fig. 3 Thermogravimetric curve of the as-prepared SC sample via the solvothermal reaction at 180 °C for 24 h

tin elements, as shown in Fig. 2. The atomic ratio of the carbon in the as-prepared SC sample was about 65%, estimated from the EDS result.

TGA analysis

Figure 3 shows thermogravimetric curve of the as-prepared SC sample. From TGA measurements, it is seen that the as-prepared SC decomposes in two steps. The first step occurs between 100 and 600 °C in the TGA curve, the weight loss in this step is 18.9%. This weight loss could be attributed to the evaporation of physically absorbed water and residual solvent in the samples. In the second step, a condensation process occurs and more water molecule is released from 600 to 800 °C. From 800 °C onwards, a gradual continuous mass loss takes place, due to the reduction of SnO_2 to Sn by carbon [17].

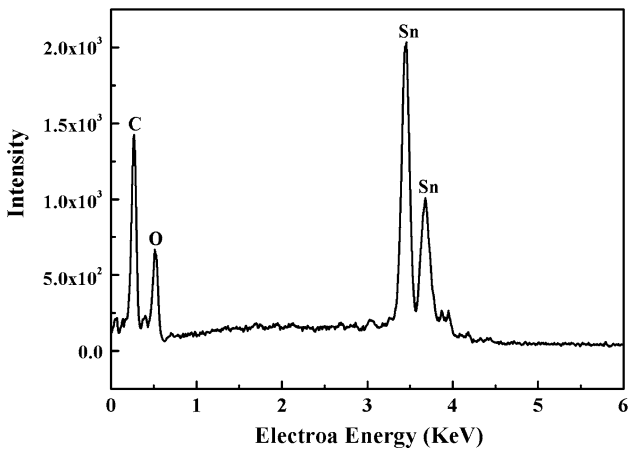

Fig. 2 EDS spectrum of the as-prepared SC sample via solvothermal reaction at 180 °C for 24 h

XPS spectra

X-ray photoelectron spectroscopy was used to investigate the surface chemical composition of the resulting sample. XPS survey spectrum of the as-prepared SC sample confirms that the sample contains only Sn, O, and C (Fig. 4a). And binding energies for Sn $3d_{5/2}$, O 1s, and C 1s are 485.4, 531.0, and 284.4 eV, respectively. The core level spectra of C 1s and O 1s regions were also investigated by XPS. The broad peak of C 1s can be fitted by two peaks at the binding energies of 284.4 and 286.5 eV for the as-prepared SC sample (Fig. 4b). The dominant peak (284.4 eV) is thought to signal the presence of elemental carbon and the peak (286.5 eV) indicates the presence of C–O bonds. Such strong signal of elemental carbon should not only arise from adventitious carbon, but also from the carbon reduced from glucose. Moreover, the broad peaks of O 1s can be fitted by two peaks at binding energies of 531.0 and 533.2 eV (Fig. 4c), corresponding to oxygen in metal oxides and carbonate species, respectively. XPS signals of Sn 3d were observed at binding energies at around 485.4 (Sn $3d_{5/2}$) and 495.1 eV (Sn $3d_{3/2}$) (Fig. 4d), suggesting the existence of SnO_2.

IR analysis

The IR spectrum was used to identify the functional groups present after solvothermal treatment. The infrared spectrum of as-prepared SC sample is shown in Fig. 5. Dehydration

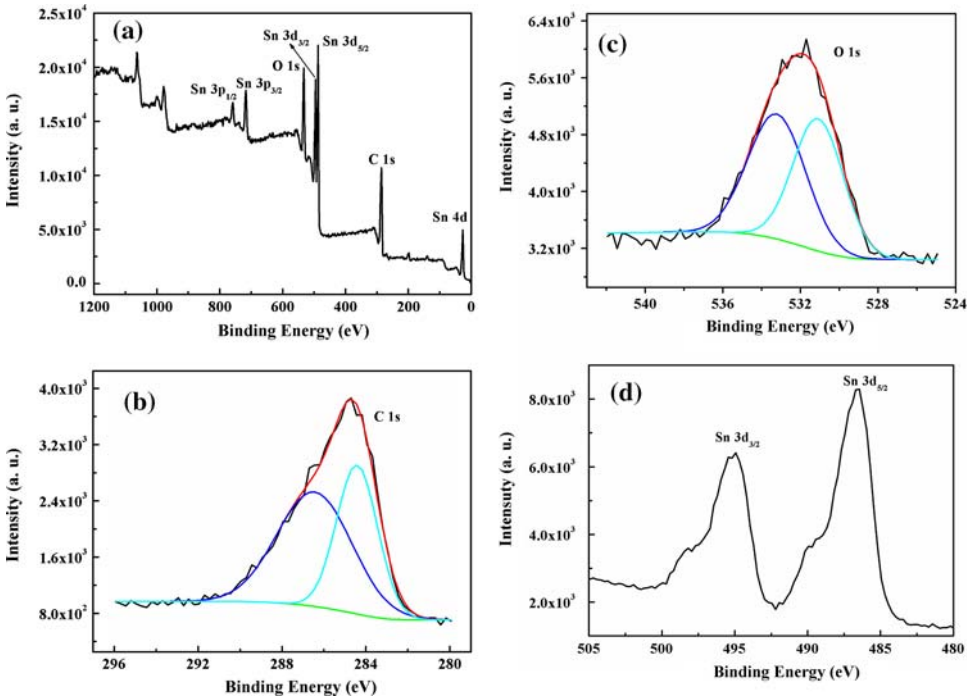

Fig. 4 XPS spectra of the as-prepared SC sample: (**a**) survey spectrum, (**b**) C 1s, (**c**) O 1s, and (**d**) Sn 3d

and aromatization are usually regarded as a process of decreasing the number of functional groups [27]. The bands at 1710 and 1620 cm^{-1}, attributed to C=O and C=C vibrations, respectively, suggest the aromatization of glucose during solvothermal treatment. The bands appearing in the 1000–1300 cm^{-1} spectral region, which include the C–OH stretching and OH bending vibrations, imply the existence of large numbers of residual hydroxyl groups. In these partially dehydrated residues of the as-prepared SC sample, reductive OH or CHO groups are covalently bonded to the carbon frameworks to improve the hydrophilicity and stability of the as-prepared SC sample in aqueous solutions, and thus make it potential for hybrid core-shell structure or hollow/porous materials [28].

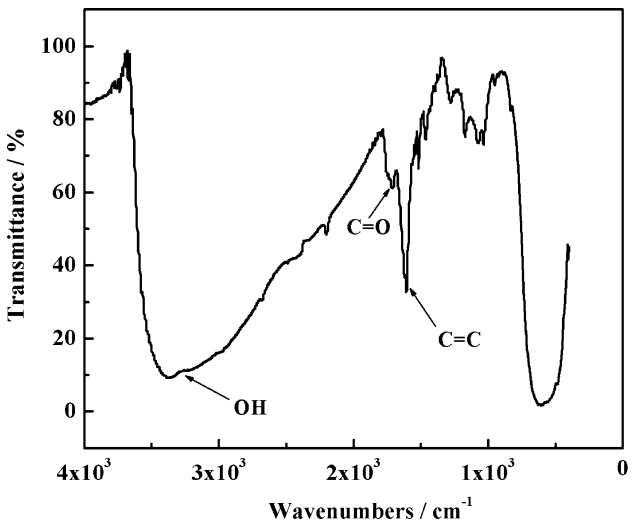

Fig. 5 IR spectra of the as-prepared SC sample via the solvothermal reaction at 180 °C for 24 h

SEM and TEM images

The morphologies of the resulting samples were investigated by field-emission scanning electron microscopy. SEM observation reveals that the as-prepared SC sample consists of spherical particles (Fig. 6a). The sizes of these spheres were not uniform. Their diameters were in the range of 1–2 μm. The surfaces of these spheres were relatively smooth. A typical TEM image (Fig. 6b) further confirms the spherical morphology of the as-prepared SC sample. Figure 6c shows the TEM image of the annealed SC sample. The spherical morphology of the sample was kept well after annealing. The sizes of the annealed SC spheres are 200–400 nm, significantly smaller than those of the as-prepared SC sample. Interestingly, some core-shell structured microspheres were formed. Because heavier SnO_2 possess darker contrast than C under TEM e-beam, it is believed that the microspheres consist of SnO_2 cores and C shells. The sizes of these SnO_2 cores are in the range of 100–300 nm. Besides SnO_2@C core-shell spheres, some carbon spheres without SnO_2 cores are also observed.

Formation of SnO_2@C core-shell spheres

Hyeon and coworkers synthesized hollow tin dioxide (SnO_2) microspheres by the heat treatment of a mixture

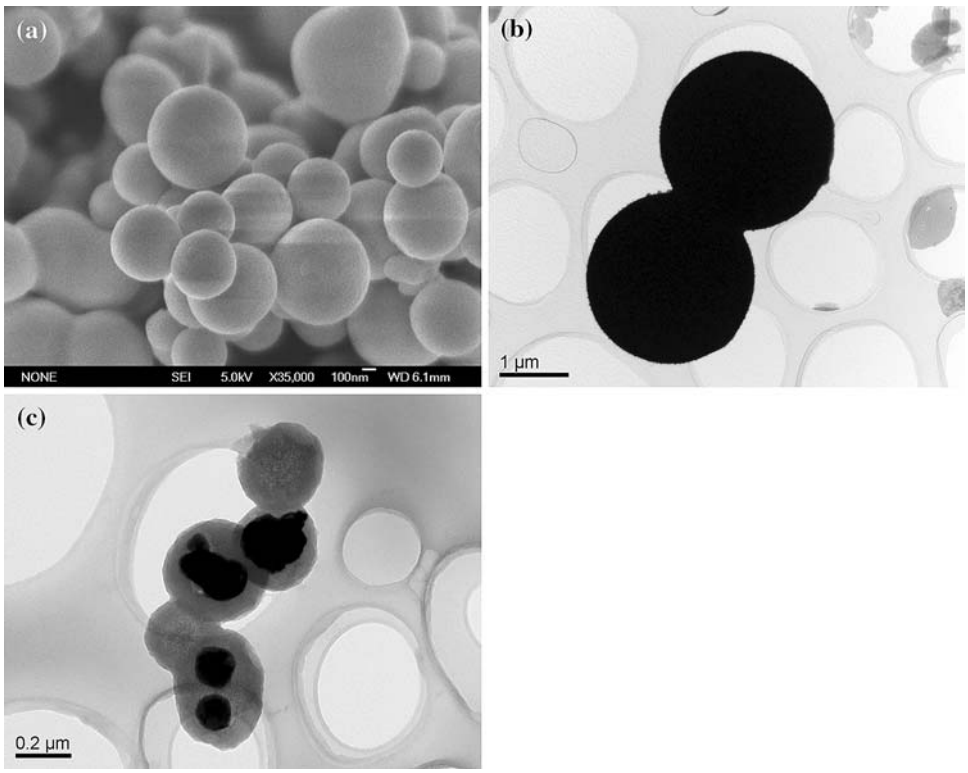

Fig. 6 FE-SEM (**a**) and TEM (**b**) image of the as-prepared SC sample; and TEM (**c**) image of the annealed SC sample

composed of tin(IV) tetrachloride pentahydrate and resorcinol–formaldehyde gel [29]. They found that micrometer-sized spherical particles are known to form in the low pH condition. In our study, the initial pH value of the reaction mixture of tin(II) chloride and glucose was 1.2. It seems that this pH also favors the formation of micrometer-sized dense spherical particles.

Various chemical reactions of glucose can take place under hydro(solvo)thermal conditions and result in a complex mixture of organic compounds [11, 21, 27, 30]. This makes it difficult to determine the exact chemical reaction in the sealed vessel. We found that no solid products were formed if only glucose was solvothermally treated in absence of metal salts. Moreover, hybrid spheres of SC could not be obtained in cases of solvothermal treatment below 140 ^{o}C or at 180 ^{o}C for less than 2 h. In those cases, the formation of viscous solution with an olive-drab color indicates that some aromatic compounds and oligosaccharides were formed. This process was denoted as "polymerization" by other researchers [27]. In our study, the solvothermal reaction would induce the polymerization process of glucose. During the polymerization, the functional groups of glucose would be broken to produce some organic compounds with lower polarity in the solution. These organic compounds became water-insolubles, but ethanol-soluble. The ethanol-soluble species may be the intermediates for the subsequent formation of as-prepared SC sample at higher temperatures and after longer reaction time. When the temperature was higher than 140 ^{o}C or the reaction time was longer than 2 h at 180 ^{o}C, the ethanol-soluble intermediates were converted to the as-prepared SC sample, in which tin compounds (or amorphous tin oxide) were packed in the carbonaceous spheres.

Based on the above results, we proposed a possible pathway for the formation of SnO_2@C core-shell spheres. This pathway involves the first formation of aromatic compounds containing tin ions through polymerization and the subsequent formation of hybrid spheres through the simultaneous solvothermal carbonization and precipitation of amorphous tin compounds (or amorphous tin oxide), and the final formation of SnO_2@C core-shell spheres by annealing at 600 ^{o}C in a high-purity nitrogen atmosphere. Obviously, aggregation of nanoparticles took place during the transformation of amorphous tin compounds (or amorphous tin oxide) into crystalline SnO_2. This aggregation produced the SnO_2 cores in the microspheres.

Charge–discharge test

It is well known that both SnO_2 and hard carbon from glucose are Li storage materials [29, 31]. The SnO_2 anode has a theoretical specific capacity of 790 mAh/g, which is much higher than that of graphite (372 mAh/g) [1, 2]. However, its commercial use was hindered by their drastic

volume change during Li insertion/extraction cycles, which leads to fast capacity fading [20, 32]. Tin oxide composite materials can overcome the drastic volume change during Li insertion/extraction cycles [33]. The reaction mechanism was that lithium first reacts with tin oxide to produce amorphous Li_2O and Sn irreversibly, and then Sn alloys with Li reversibly [6, 34, 35]. The Li_2O matrix acts as a buffer and dispersive medium for nanosized Sn grains, which is critical for improving the cycling performance. Meanwhile, besides carbon, inactive glass-forming elements such as B or P can also act as a buffer to improve the cycling performance [33, 36, 37]. Li and coworkers proposed the reaction mechanism of the SnO_2@C composite as follows [21]:

$$2Li^+ + SnO_2 + 2e^- \rightarrow Li_2O + Sn \quad (1)$$

$$xLi^+ + Sn + xe^- \rightarrow Li_xSn \quad (x \leq 4.4) \quad (2)$$

$$yLi^+ + C_6 + ye^- \leftrightarrow Li_yC_6 \quad (y \leq 4.4) \quad (3)$$

It is obvious that if the buffer medium itself has Li storage capacities and high electronic conductivity, the capacity of tin oxide composite anodes could be further enhanced. The carbonaceous matrix from glucose was demonstrated to be an excellent candidate to realize this ideal [31, 38].

Figure 7 shows the charge and discharge curves of SnO_2@C core-shell spheres and the corresponding variation of discharge capacity vs. cycle number at a constant current of 30 mA/g with a cutoff voltage window of 1.2 and 0.01 V vs. Li^+/Li. Figure 7a shows that the initial discharge and charge capacity is 667.4 and 518.3 mAh/g, respectively. The large irreversible capacity loss during first lithiation process may be attributed to the irreversible equation (1) and solid electrolyte interface (SEI) formation [3, 39]. Whereas, the coulombic efficiency was observed to increase from the initial value of 78% to 97% in the third cycle. Figure 7b shows the discharge capacity vs. cycle number. The capacity decreased with the increase of the cycle numbers and reached a very stable reversible capacity at about 370 mAh/g only after 18 cycles. Though the SnO_2@C core-shell spheres synthesized in this study was much lower than that of the previous report (about 1600 mAh/g) [21], it exhibited an improved cycle performance. In that study, the SnO_2@C core-shell nanostructure still inclined to decay even after 30 cycles [21]. Some previous studies on SnO_2 anode provided some hints to explain this rapid stabilization ability [18, 40]. It has been reported that transition metal oxides show reversible Li storage behaviors [41, 42]. In those cases, a transition metal can react with Li_2O upon Li extraction, driving Eq. 1 reversible. This contributes to the high reversible capacity. Meanwhile, a previous study mentioned that Li–O bonds were not stable when the charging voltage is above 1.3 V

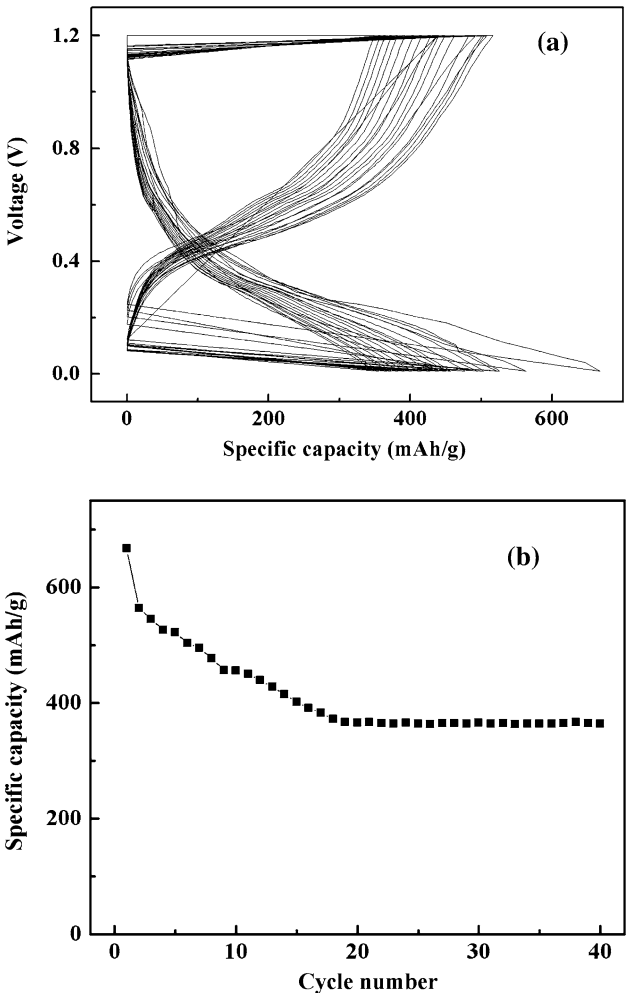

Fig. 7 The charge and discharge curves (**a**) and variation of discharge capacity vs. cycle number (**b**) of the annealed SnO_2@C core-shell spheres

[6]. Moreover, a recent work indicated that reaction (1) could be thermodynamically reversible for most of the metal compounds [43]. For the SnO_2@C core-shell spheres, the SnO_2 cores are embedded in the carbon shells, which ensure the formed Li_2O and Sn contact well without separation. Meanwhile, the carbonaceous matrix (the shell) has Li storage capacity and high electronic conductivity. It has the ability to keep SnO_2 cores electrically connected and stabilize the SnO_2 cores against agglomeration during charging–discharging process. These factors significantly improved the cycling performance of SnO_2@C core-shell spheres.

Conclusions

In this study, we synthesized SnO_2@C core-shell spheres as anodes of lithium ion batteries. Electrochemical performance

test showed that SnO_2@C core-shell spheres exhibited an initial discharge specific capacity of 667.4 mAh/g and a stabilized capacity at 366.4 mAh/g after 18 cycles in the potential range of 1.2–0.01 V. The improved cycling performance could be attributed to the carbon shells, which can enhance the conductivity of SnO_2 cores and suppress the aggregation of active particles during cycling. These SnO_2@C core-shell spheres are promising anodes for lithium-ion batteries. This study provides a facile way to improve the cycle ability of transition oxides for reversible lithium-ion storage.

Acknowledgements This work was supported by National Basic Research Program of China (973 Program) (Grant 2007CB613301), National Science Foundation of China (Grants 20503009, 20673041, and 20777026), and Program for New Century Excellent Talents in University (Grant NCET-07-0352).

References

1. Wu YP, Rahm E, Holze R (2003) J Power Sources 114:228
2. Buqa H, Goers D, Holzapfel M, Spahr ME, Novak P (2005) J Electrochem Soc 152:A474
3. Winter M, Besenhard JO, Spahr M, Novak P (1998) Adv Mater 10:725
4. Winter M, Besenhard JO (1999) Electrochim Acta 45:31
5. Li N, Martin CR (2001) J Electrochem Soc 148:A164
6. Courtney IA, Dahn JR (1997) J Electrochem Soc 144:2943
7. Wang GX, Yao J, Liu HK, Dou SX, Ahn JH (2004) Electrochim Acta 50:517
8. Fan J, Wang T, Yu C, Tu B, Jiang Z, Zhao D (2004) Adv Mater 16:1432
9. Wang Y, Lee JY (2004) J Phys Chem B 108:17832
10. Wang Y, Lee JY, Zeng HC (2005) Chem Mater 17:3899
11. Noh M, Kwon Y, Lee H, Cho J, Kim Y, Kim MG (2005) Chem Mater 17:1926
12. Lou XW, Wang Y, Yuan C, Lee JY, Archer LA (2006) Adv Mater 18:2325
13. Wang Y, Su FB, Lee JY, Zhao XS (2006) Chem Mater 18:1347
14. Zhu JJ, Lu ZH, Aruna ST, Aurbach D, Gedanken A (2000) Chem Mater 12:2557
15. Park MS, Wang GX, Kang YM, Wexler D, Dou SX, Liu HK (2007) Angew Chem Int Ed 46:750
16. Kim C, Noh M, Choi M, Cho J, Park B (2005) Chem Mater 17:3297
17. Read J, Foster D, Wolfenstine J, Behl W (2001) J Power Sources 96:277
18. Wang Y, Lee JY (2003) Electrochem Commun 5:292
19. Yuan L, Konstantinov K, Wang GX, Liu HK, Dou SX (2005) J Power Sources 146:180
20. Lee KT, Jung YS, Oh SM (2003) J Am Chem Soc 125:5652
21. Sun XM, Liu JF, Li YD (2006) Chem Mater 18:3486
22. Wang GX, Ahn JH, Yao J, Bewlay S, Liu HK (2004) Electrochem Commun 6:689
23. Wen ZS, Yang J, Wang BF, Wang K, Liu Y (2003) Electrochem Commun 5:165
24. Fu LJ, Liu H, Zhang HP, Li C, Zhang T, Wu YP, Holze R, Wu HQ (2006) Electrochem Commun 8:1
25. Huang XH, Tu JP, Zhang CQ, Chen XT, Yuan YF, Wu HM (2007) Electrochim Acta 52:4177
26. Huang XH, Tu JP, Zhang CQ, Xiang JY (2007) Electrochem Commun 9:1180
27. Sakaki T, Shibata M, Miki T, Hirosue H, Hayashi N (1996) Bioresour Technol 58:197
28. Hans ML, Lowman AM (2002) Curr Opin Solid State Mater Sci 6:319
29. Han SJ, Jang B, Kim T, Oh SM, Hyeon T (2005) Adv Funct Mater 15:1845
30. Peng Q, Dong YJ, Li YD (2003) Angew Chem Int Ed 42:3027
31. Wang Q, Li H, Chen LQ, Huang X (2002) J Solid State Ionics 152:43
32. Yang J, Winter M, Besenhard JO (1996) Solid State Ionics 90:281
33. Idota Y, Kubota T, Matsufuji A, Maekawa Y, Miyasaka T (1997) Science 276:1395
34. Liu WF, Huang XJ, Wang ZX, Li H, Chen LQ (1998) J Electrochem Soc 145:59
35. Li H, Huang XJ, Chen LQ (1998) Electrochem Solid State Lett 1:241
36. Hayashi A, Nakai M, Tatsumisago M, Minami T, Katadab M (2003) J Electrochem Soc 150:A582
37. Wan KB, Li SFY, Gao ZQ, Siow KS (1998) J Power Sources 75:9
38. Xing WB, Dunlap RA, Dahn JR (1998) J Electrochem Soc 145:62
39. Grugeon S, Laruelle S, Herrera-Urbina R, Dupont L, Poizot P, Tarascon J-M (2001) J Electrochem Soc 148:A285
40. Zhang R, Lee JY, Liu ZL (2002) J Power Sources 112:596
41. Poizot P, Laruelle S, Grugeon S, Dupont L, Tarascon J-M (2000) Nature 407:496
42. Poizot P, Laruelle S, Grugeon S, Dupont L, Tarascon J-M (2001) J Power Sources 97–98:235
43. Li H, Balaya P, Maier J (2004) J Electrochem Soc 151:A1878